NANO LETTERS

2007
Vol. 7, No. 11
3349−3354

Formation of Single-Walled Carbon Nanotube via the Interaction of Graphene Nanoribbons: Ab Initio Density Functional Calculations

A. J. Du,[†,‡] Sean C. Smith,[*,†,‡] and G. Q. Lu[‡]

Centre for Computational Molecular Science and ARC Centre for Functional Nanomaterials, Australian Institute for Bioengineering and Nanotechnology, The University of Queensland, QLD 4072, Brisbane, Australia

Received July 4, 2007; Revised Manuscript Received September 9, 2007

ABSTRACT

The interaction of bare graphene nanoribbons (GNRs) was investigated by ab initio density functional theory calculations with both the local density approximation (LDA) and the generalized gradient approximation (GGA). Remarkably, two bare 8-GNRs with zigzag-shaped edges are predicted to form an (8, 8) armchair single-wall carbon nanotube (SWCNT) without any obvious activation barrier. The formation of a (10, 0) zigzag SWCNT from two bare 10-GNRs with armchair-shaped edges has activation barriers of 0.23 and 0.61 eV for using the LDA and the revised PBE exchange correlation functional, respectively. Our results suggest a possible route to control the growth of specific types SWCNT via the interaction of GNRs.

Since the discovery of fullerenes and carbon nanotubes, low-dimensional nanoscale carbon materials have been the subject of intensive research during the past 2 decades due to the peculiar electronic structures that are expected to be important for practical applications in nanoelectronics.[1,2] Recently, single graphite layers, referred to as graphene nanoribbons (GNRs) have been prepared experimentally by using conventional device setup.[3,4] Moreover, methods such as mechanically cutting exfoloiated graphenes[5,6] or patterning epitaxially grown graphenes[7] have been also developed for realizing varying widths of GNRs. Such findings have opened up exciting opportunities for the design of novel electronic devices and interconnects, e.g., quantum information processing,[8] tiny transistors,[4,9] and so on. Theoretically, there have been many existing studies to predict the band ferromagnetism,[10−12] the energy gaps,[13] and optical properties[14] of GNRs with various widths. These provided a qualitative way of determining the electronic properties of ribbons with widths of practical significance. More recently, results obtained in the Berkeley lab show that zigzag GNRs are magnetic and can carry a spin current response to the external electric field. This opens a new path to the application of spintronics.[15]

Generally, single-walled carbon nanotubes (SWCNTs) are typically grown as mixtures of metallic and semiconducting tubes, depending on the arrangement of the hexagonal rings along the tubular surface.[16] However, this actually constitutes one of the notable obstacles to the widespread application of this unique material, since metallic and semiconducting materials have very different functions in nanodevices. Hence, separating them has become a central issue in terms of effective fabrication of high-performance electronic devices. Currently, many physical and chemical methods have been developed for the separation according to the respective electronic properties by using dielectrophoresis,[17,18] selective flocculation,[19] selective adsorption of the functional group,[20,21] and density gradient induced centrifugation.[22] However, none of these is satisfactory from the point of view of high throughput, better selectivity and yield, and more favorable scalability.[23]

Recently, the "partial radical" concept for GNRs with zigzag-shaped edge has been proposed by Jiang et al.[24] due to the strong localized state near the Fermi level. Bare GNR also has unsaturated dangling bonds at zigzag or armchair-shaped edges. Clearly a single graphene sheet is very difficult to roll into a SWCNT without any catalyst. An intriguing question, however, is whether it is possible to form SWCNTs via the interaction of bare GNRs? To explore this question, we report below a series of calculations to study the

* Corresponding author. E-mail: s.smith@uq.edu.au.
† Centre for Computational Molecular Science.
‡ ARC Centre for Functional Nanomaterials.

10.1021/nl071613d CCC: $37.00
Published on Web 10/10/2007

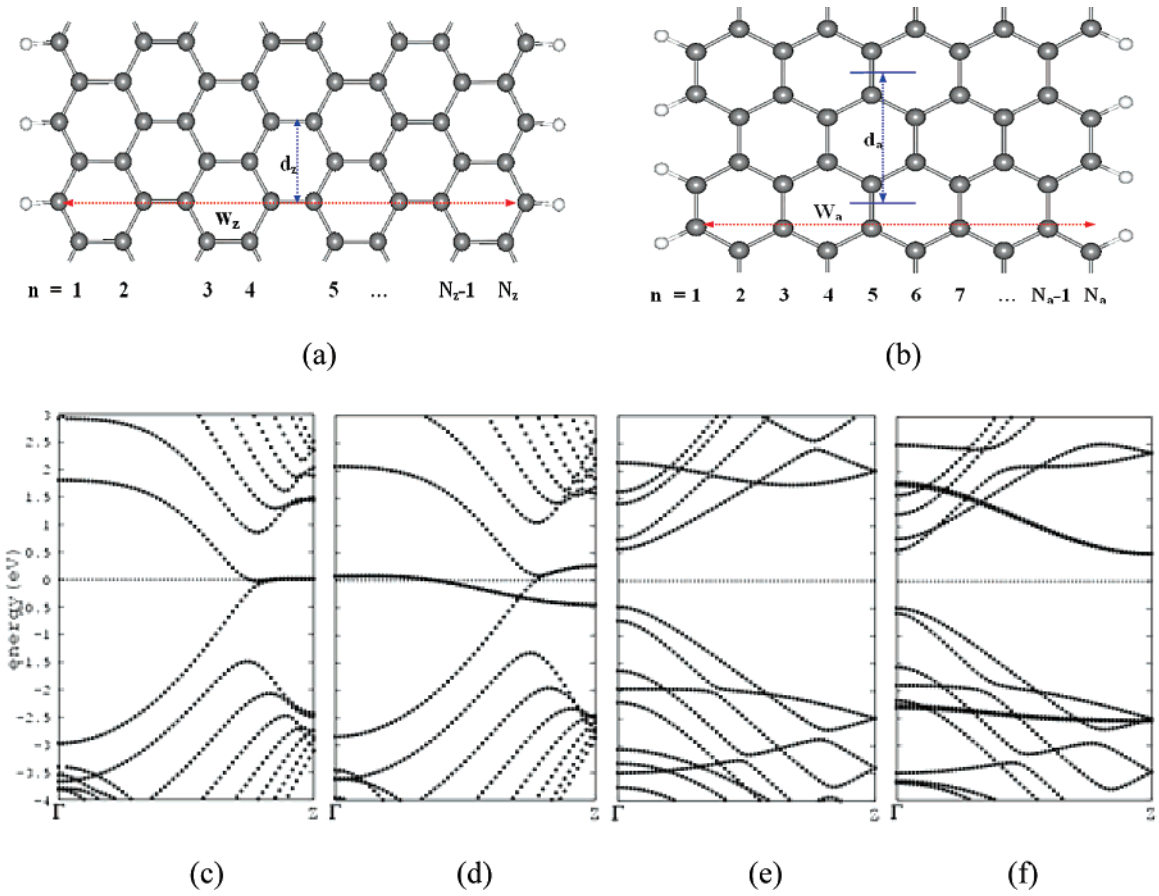

Figure 1. Geometry structure for hydrogen-terminated graphene nanoribbons (GNRs) with (a) zigzag- and (b) armchair-shaped edges. (c) and (e) represent the corresponding band structures for (a) and (b), respectively. (d) and (f) present the band structure of bare 8-ZGNR and 10-AGNR, respectively. The gray and white balls represent C and H atoms, respectively. The Fermi level was indicated as the dashed line at $E = 0$ eV. The 1D unit cell distance and the ribbon width are denoted by $d_z(d_a)$ and $W_z(W_a)$ for 8-ZGNR (10-AGNR).

interaction of bare GNRs with both armchair- and zigzag-shaped edges. We found that two bare nanoribbons ($N_z = 8$) with zigzag-shaped edge could form a (8, 8) single-wall armchair carbon nanotube with almost no activation barrier. In contrast, there is a significant activation barrier for the formation of a (10, 0) single-wall zigzag nanotube from armchair-shaped ribbons ($N_a = 10$), suggesting a possible route for selective synthesis and growth of nanotubes with specific properties via the interaction of GNRs.

Computational Details. All the calculations were performed by using the plane-wave basis VASP code[25,26] implementing both local density approximation (LDA) and the generalized gradient approximation (GGA) (revised PBE exchange correlation functional).[27−29] An all-electron description, the projector augmented wave method (PAW)[30,31] is used to describe the electronic-ion-core interaction. The cutoff energies for plane waves are chosen to be 500 eV, and the supercell is large enough to ensure that the vacuum space is at least 16 Å, which is enough to separate the interaction between periodic images. Monkhost pack mesh of K-points ($1 \times 1 \times 7$) is used for sampling the one-dimensional Brillium zone during geometry optimization with 0.01 eV/Å convergence tolerance of force on each atom. The accurate band structure calculations are based on LDA only by using 60 k-points along the Z axis.

To determine activation barriers for the formation of armchair- and zigzag-type nanotube via the interaction of GNRs with zigzag- and armchair-shaped edge, the nudged elastic band (NEB) method was used.[32,33] This method involves optimizing a chain of images that connect the reactant and product state. Each image is only allowed to move into the direction perpendicular to the hypertangent. Hence the energy is minimized in all directions except for the direction of the reaction path. A damped molecular dynamics was used to relax ions until the force in each image is less than 0.02 eV/Å. We note that the contribution from spin polarization is not included in our calculation due to reasons of computational feasibility.

Results and Discussion. Following the previous convention by Son et al.,[10] the GNRs with zigzag-shaped edge on both sides (ZGNR) are classified by the number of zigzag chains (N_z) across the ribbon width as shown in Figure 1a. Likewise, GNRs with armchair-shaped edge on both sides (AGNR) are classified by the number of dimer lines (N_a) across the ribbon width (see Figure 1b). 8-ZGNR and 10-AGNR represent GNR with 8 zigzag chains and 10 dimer lines, respectively. First, geometry optimizations for 8-ZGNR and 10-AGNR with and without H-termination were performed utilizing the conjugate gradient method. The band structures for 8-ZGNR and 10-AGNR with and without

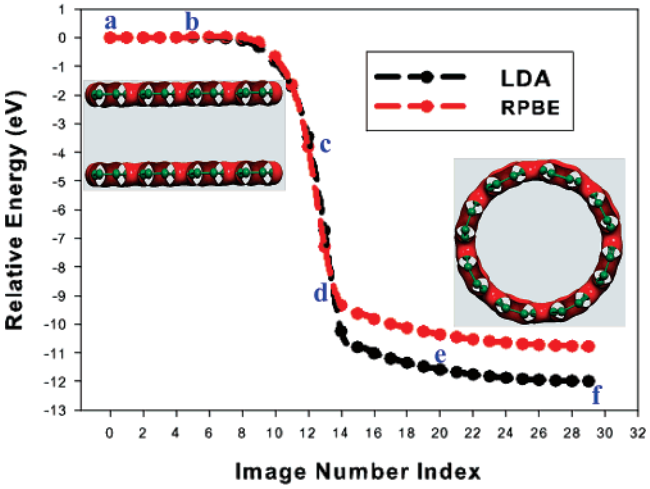

Figure 2. The calculated energy profile for the formation of a (8, 8) armchair single-wall carbon nanotube via the interaction of two bare 8-ZGNRS based on LDA and GGA (RPBE), respectively. a, b, c, d, e, and f correspond to the IS, 5th image, TS, 11th image, 21st image, and FS along the minimum energy pathway, respectively.

H-saturation were calculated and are plotted in parts c−f of Figure 1, respectively. Clearly, the localized edge state appears around the Fermi level for H-terminated 8-ZGNR and a direct gap (0.9 eV) is observed for H-terminated 10-AGNR (see parts c and e of Figure 1). Collectively, they are in good agreement with other recent theoretical studies.[14] Additionally, a degenerate and very flat band appears in the bare 8-ZGNR and 10-AGNR (without H-termination at both sides). These represent carbon dangling bonds at the edges, since each edge carbon atom is only bound to two neighboring carbon atoms. The difference between them is that the electronic state is half occupied and strongly localized around the Fermi level in 8-ZGNR, which may imply a high chemical reactivity.

Recently, the "partial radical" concept for ZGNRs has been proposed by Jiang et al.[24] Apparently, the existence of dangling carbon bonds in the bare GNR should offer a much higher chemical reactivity to manipulate the interaction of GNRs. This prompts the question as to whether we could form a SWCNT via the bare GNRs. To search for a possible pathway by which this might happen, we first position two bare 8-ZGNRs at a large separation distance (5 Å) as the initial state (IS), such that the interaction between them is very weak. A pristine (8, 8) armchair SWCNT is formed as the final state (FS). Then a chain of images (28) is laid between the IS and the FS and the NEB algorithm is used to minimize the appropriate effective force acting on each image. The energy profiles for the final minimum energy pathway (MEP) between the IS and the FS, as well as a three-dimensional isosurface of electronic charge density (in red) for the IS and FS, are plotted in Figure 2.[34] The activation barriers (0.01 and 0.05 eV for LDA and GGA (RPBE) calculation, respectively) are negligible.[35] Clearly, the (8, 8) armchair SWCNT could be easily formed via the interaction of two bare 8-ZGNRs. This can be understood by the strongly localized electronic state across the Fermi level at the zigzag edges as alluded to above (see Figure 1d). To study the

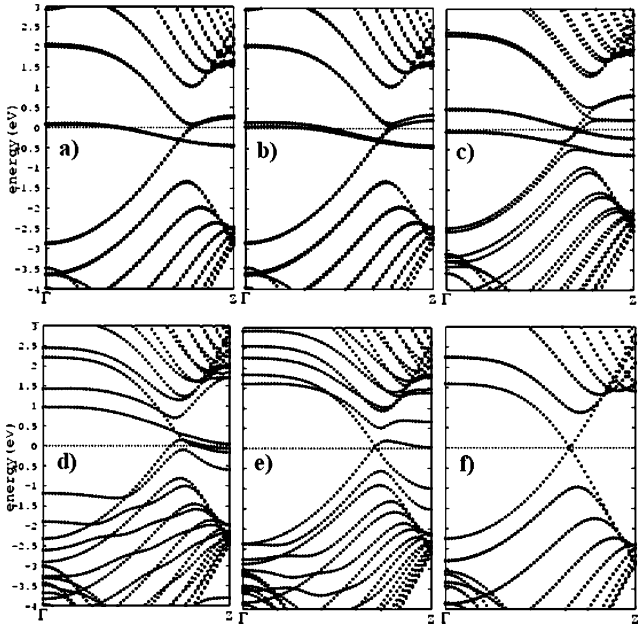

Figure 3. The corresponding band structures (LDA only) for the chosen images along MEP as indicated by a, b, c, d, e, and f in Figure 2. The dashed line at $E = 0$ eV represents the Fermi level.

influence of temperature, we have performed molecular dynamics (MD) simulation at 300 K for two 8-ZGNRs positioned at a distance of 3.3 Å, which is very close to the natural separation of two graphite layers. Our MD simulation was based on the canonical (NVT) ensemble and contained totally 1600 carbon and 32 H atoms. The second-generation reactive empirical bond order potential[36] with 6-12 Lennard-Jones correction at long distance was used to describe the C−C and C−H interaction. As would be expected on the basis of the computed MEPs, (8,8) armchair SWCNTs can be formed around 160 ps (see Supporting Information). This indicates the barrier should be very small if there is any and thus confirmed our NEB path. In Figure 3, we present a series of band structures for some chosen images (a, b, c, d, e, and f sites as shown in Figure 2) along the minimum energy pathway. Figure 3a is similar to Figure 1c and corresponds to two 8-ZGNRs separated at far distance. Figure 3f shows the band structure for a pristine (8, 8) armchair SWCNT. Clearly the metallic behavior and the $\pi-\pi^*$ band crossing can be seen near the BZ boundary (Z-point).[37] As shown in parts b−e of Figure 3, the charge density starts to overlap at edge when two 8-ZGNRs move closer to each other. The degenerate, half-occupied flat band near the Fermi level (see Figure 3a) will split. Finally, the $\pi-\pi^*$ band crossing almost comes into form and the metallic behavior of armchair SWCNT can be seen clearly even in the 21st image (see Figure 3e).

Subsequently, we then turn to study the interaction of two bare 10-AGNRs (see Figure 1b). The NEB calculation is very similar to the above calculations, but for the formation of a (10, 0) zigzag SWCNT. Figure 4a presents the energy profile along the MEP from 10-AGNRs to a semiconducting (10, 0) SWCNT by using both the LDA and GGA (RPBE) exchange correlation functional, respectively. Parts b and c of Figure 4 show the activation barriers of Figure 4a with a

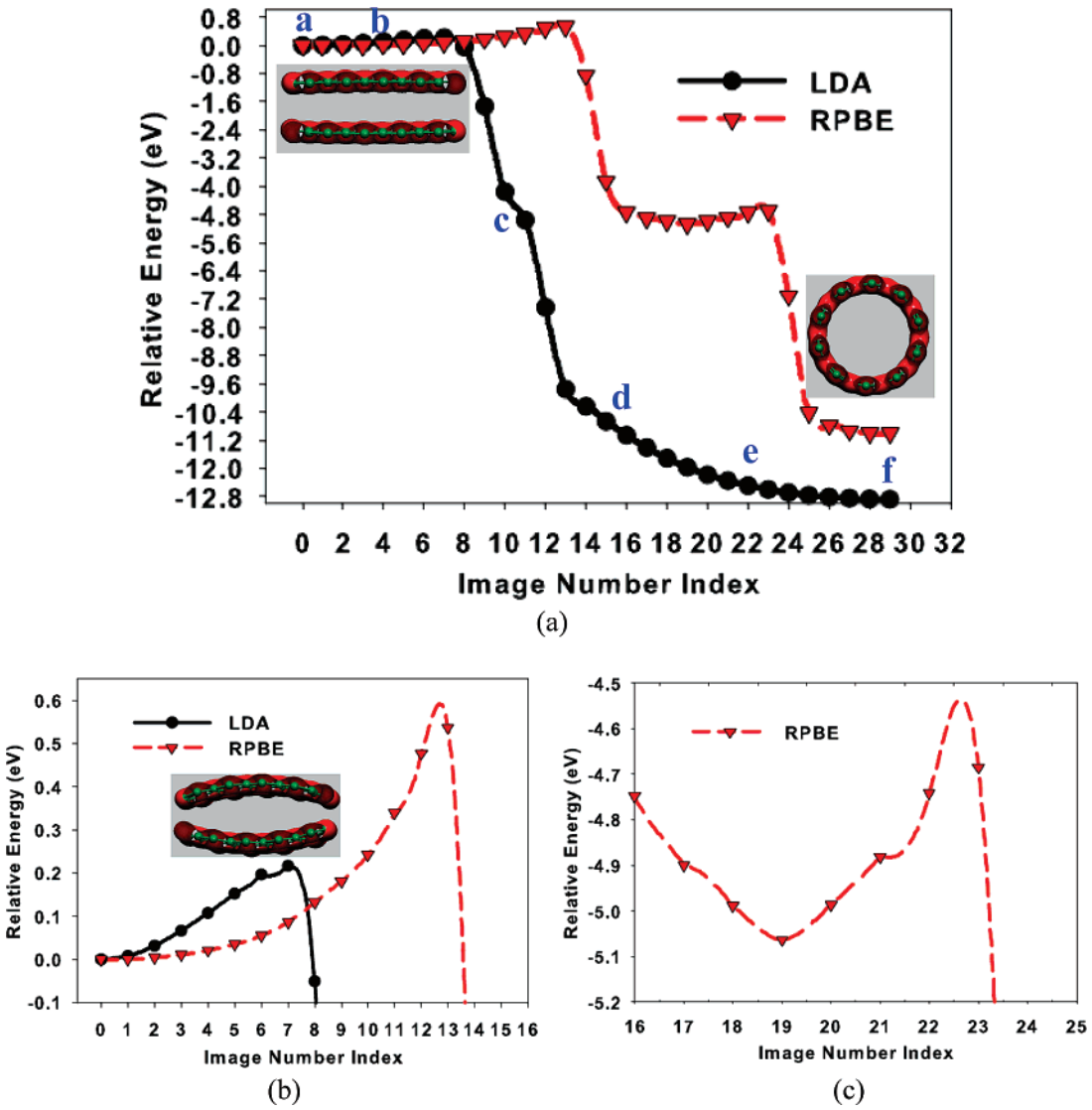

Figure 4. (a) The calculated energy profile for the formation of a (10, 0) zigzag semiconducting single-wall carbon nanotube via the interaction of two bare 10-AGNRs based on LDA and revised PBE exchange correlation functional, respectively. a, b, c, d, e, and f correspond to the IS, 5th image, TS, 11th image, 22nd image, and FS along the minimum energy pathway, respectively. Cutouts (b) and (c) show the barriers from Figure 4a on a larger scale.

larger scale. In strong contrast to the former calculation, the effective activation barriers for the formation of a (10, 0) SWCNT via the interaction of two 10-AGNRs are 0.23 and 0.57 eV for LDA and GGA (RPBE), respectively. An additional transition state (E_a = 0.61 eV) was also found when using the RPBE exchange correlation functional (see Figure 4c). A careful check of the transition states shows that calculations based on RPBE give two-step chemical reactions. The first step corresponds to the bonding at one end of two 10-AGNRs and the second step involves binding at the other end of the 10-AGNRs (see movie files in the Supporting Information). Clearly, the above results indicate a rate-limiting process during the formation of (10, 0) SWCNT via the bare 10-AGNRs, contrasting with the formation of (8, 8) armchair SWCNT via 8-ZGNRs. The possible reason for this could be that the degenerate band is far from the Fermi level in 10-AGNRs, whereas it is strongly localized around the Fermi level for 8-ZGNRs. Figure 5 presents a series of band structures for some chosen images (a, b, c, d, e, and f sites as shown in Figure 4) along the MEP. Figure 5a actually corresponds to the IS (two 10-AGNRs at far distance) and the degenerated band can be seen clearly there. Figure 5f shows a typical semiconducting band strucure for (10, 0) SWCNT with a band gap of 0.9 eV, which is in good agreement with ref 38. The degenerated band appearing in an unoccupied state will split as shown from Figure 5b to Figure 5e as two 10-AGNRs move closer. Only one split band moved across the Fermi level and finally became occupied (see Figure 5b−d). A (10, 0) zigzag semiconducting SWCNT was formed almost at image 22 as shown in Figure 5e.

In order to build reliable microelectronic nanodevices based on SWCNTs, selective processes must be developed to create SWCNTs with specific electronic and mechanical properties. Despite many experimental efforts directed toward the separation of metallic and semiconducting nanotubes,

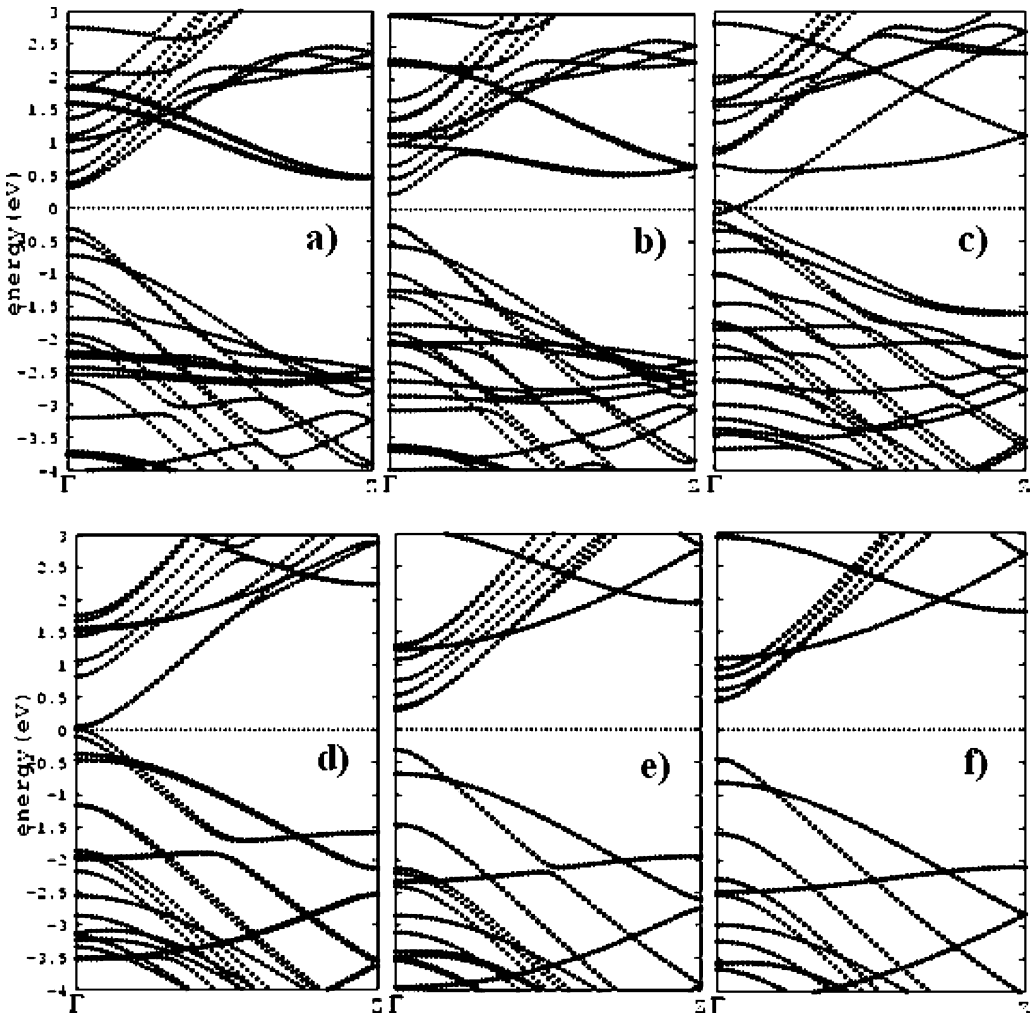

Figure 5. The corresponding band structures (LDA only) for the chosen images along the MEP as indicated by a, b, c, d, e, and f in Figure 4. The dashed line at $E = 0$ eV represents the Fermi level.

most of them are actually not selective for the diameter and chirality.[39] Furthermore, techniques such as chemical functionalization may also introduce defects and require further processing to restore the useful electronic properties of SWCNT. Hence, improved techniques are still needed. More recently, Smalley's group has developed a cloning method to cut up individual nanotubes into short segments that act as the seeds for regrowing entire tubes.[39,40] Herein we demonstrated that an (8, 8) armchair-type SWCNT can be formed via the interaction of two 8-ZGNRs with almost no activation barrier. Contrastingly, the formation of a (10, 0) zigzag-type SWCNT via the interaction of 10-AGNRs is predicted to be kinetically limited by the presence of at least one barrier. In light of exciting recent progress on the controllable growth of two-dimensional GNRs with various widths, these results suggest an alternative approach to the selective synthesis of SWCNTs with specific diameter and chiarility that may provide an interesting avenue for future investigations. It should be noted by way of a caveat that this initial study deals only with pristine grapheme nanoribbons, whereas in practice the edges may be partially oxidized, hydrogenated,[41] etc. The impact of such edge capping or functionality on the suggested scheme for SWCNT formation will require further exploration in subsequent studies.

Conclusions. In summary, the interactions of two bare GNRs with armchair- and zigzag-shaped edges were investigated by ab initio density functional theory calculations with LDA and GGA, respectively. Remarkably, two bare 8-ZGNRs could form a (8, 8) armchair SWCNT without obvious activation barrier. The activation barrier for the formation of a (10, 0) single-walled zigzag nanotube from 10-AGNRs is around 0.23 and 0.61 eV for using the LDA and revised PBE exchange correlation functional, respectively. Considering the challenges in separating metallic and semiconducting SWCNT experimentally, our results suggest a possible alternative route to selectively synthesize specific types of nanotubes via GNRs.

Acknowledgment. We acknowledge generous grants of high-performance computer time from both the Computational Molecular Science cluster computing facility at The University of Queensland and the Australian Partnership for Advanced Computing (APAC) National Facility. The authors also greatly appreciate the financial support of the Australian

Research Council and The University of Queensland through the ARC Centre for Functional Nanomaterials.

Supporting Information Available: Energy profiles with van der Waal correction and spin-polarization for the formation of (8, 8) SWCNTs via two bare 8-ZGNRs, molecular dynamics simulation details and main results for two bare 8-ZGNRs positioned at natural separation distance of graphite layers (3.3 Å), structure files (xyz format) along the MEP for the formation (8, 8) and (10, 0) SWCNTs via the interaction of two bare 8-ZGNRs and 10-AGNRs by using LDA, and revised PBE exchange correlation functional, respectively. These materials are available free of charge via the Internet at http://pubs.acs.org.

References

(1) Dresselhaus, G.; Dresselhaus, M. S.; Eklund, P. C. *Science of Fullerenes and Carbon Nanotubes: Their Porperties and Applications*; Academic: New York, 1996.
(2) Chico, L. *Phys. Rev. Lett.* **1996**, *76*, 971.
(3) Novoselov, K. S.; Geim, A. K.; Morozov, S. V.; Jiang, D.; Zhang, Y.; Dubonos, S. V.; Grigorieva, I. V.; Firsob, A. A. *Science* **2004**, *306*, 666.
(4) Geim, A. K.; Novoselov, K. S. *Nat. Mater.* **2007**, *6*, 183.
(5) Novoselov, K. S.; Geim, A. K.; Morozov, S. V.; Jiang, D.; Katsnelson, M. I.; Grigorieva, I. V.; Dubonos, S. V.; Firsov, A. A. *Nature (London)* **2005**, *438*, 197.
(6) Zhang, Y.; Tan, Y. W.; Stormer, H. L.; Kim, P. *Nature (London)* **2005**, *438*, 201.
(7) Berger, C.; Song, Z. M.; Li, X. B.; Wu, X. S.; Brown, N.; Naud, C.; Mayo, D.; Li, T. B.; Hass, J.; Marchenkov, A. N.; Conrad, E. H.; First, P. N.; de Heer, W. A. *Science* **2006**, *312*, 1191.
(8) Falko, V. *Nat. Phys.* **2007**, *3*, 151.
(9) Yan, Q. M.; Huang, B.; Yu, J.; Zheng, F. W.; Zang, J.; Wu, J.; Gu, B. L.; Liu, F.; Duan, W. H. *Nano Lett.* **2007**, *7*, 1469.
(10) Fujita, M.; Wakabayashi, K.; Nakada, K.; Kusakabe, K. *J. Phys. Soc. Jpn.* **1996**, *65*, 1920.
(11) Okada, S.; Oshiyama, A. *Phys. Rev. Lett.* **2001**, *87*, 146803.
(12) Lee, H.; Son, Y-W.; Park, N.; Han, S.; Yu, J. *Phys. Rev. B* **2005**, *72*, 174431.
(13) Son, Y. W.; Cohen, M. L.; Louie, S. G. *Phys. Rev. Lett.* **2006**, *97*, 216803.
(14) Barone, B.; Hod, O.; Scuseria, G. E. *Nano Lett.* **2006**, *6*, 2748.
(15) Son, Y. W.; Cohen, M. L., Louie, S. G. *Nature* **2006**, *444*, 347.
(16) Saito, R.; Dresselhaus, G.; Dresselhaus, M. S. *Physical Properties of Carbon Nanotubes*; Imperial College Press: London, 1998.
(17) Peng, H.; Alvarez, N. T.; Kittrell, C.; Hauge, R. H.; Schmidt, H. K. *J. Am. Chem. Soc.* **2006**, *128*, 8396.
(18) Krupke, R.; Hennrich, F.; von Lohneysen, H.; Kappes, M. M. *Science* **2003**, *301*, 344.
(19) Chattopadhyay, D.; Galeska, L.; Papadimitrakopoulos, F. *J. Am. Chem Soc.* **2003**, *125*, 3370.
(20) Strano, M. S.; Dyke, C. A.; Usrey, M. L.; Barone, P. W.; Allen, M. J.; Shan, H.; Kittrell, C.; Hauge, R. H.; Tour, J. M.; Smalley, R. E. *Science* **2003**, *301*, 1519.
(21) Hudson, J. L.; Jian, H.; Leonard, A. D.; Stephenson, J. J.; Tour, J. M. *Chem. Mater.* **2006**, *18*, 2766.
(22) Arnold, M. S.; Green, A. A.; Hulvat, J. F.; Stupp, S. I.; Hersam, M. C. *Nat. Nanotechnol.* **2006**, *1*, 60−65.
(23) Rinzler, A. G. *Nat. Nanotechnol.* **2006**, *1*, 17.
(24) Jiang, D. E.; Sumpter, B. G.; Dai, S. *J. Chem. Phys.* **2007**, 126, 134701.
(25) Kresse, G.; Furthmuller, J. *Comput. Mater. Sci* **1996**, *6*, 15.
(26) Kresse, G.; Furthmuller, J. *Phys. Rev. B* **1996**, *54*, 11169.
(27) Ceperley, D. M.; Alder, B. J. *Phys. Rev. Lett.* **1980**, *45*, 566.
(28) Perdew, J. P.; Burke, K.; Ernzerhof, M. *Phys. Rev. Lett.* **1996**, *77*, 3865.
(29) Hammer, B.; Hansen, L. B.; Nørskov, J. K. *Phys. Rev. B* **1999**, *59*, 7413.
(30) Blochl, P. E. *Phys. Rev. B* **1994**, *50*, 17953.
(31) Kresse, G.; Joubert, D. *Phys. Rev. B* **199**9, 59, 1758.
(32) Jónsson, H. *J. Chem. Phys.* **2000**, *113*, 9978.
(33) Henkelman, G.; Uberuaga, B. P.; Jónsson, H. *J. Chem. Phys.* **2000**, *113*, 9901.
(34) In Figure 2, the relative energies to each initial state for LDA and RPBE calculations were used. Therefore the curves for LDA and PBE have the same staring point. This does not mean the total energies for LDA and PBE exchange correlation functional are the same. The same rules were used in Figure 4.
(35) A London dispersion term was incorporated into DFT as used earlier (*Nanotechnology* **2005**, *16*, 2118), and we found the effect of van der Waal correction for the activation barrier should be minor. Additionally, we also explored the effect of spin polarization and found that the energy profile and activation barrier were not affected by incorporating the spin polarization although it may lower the total energy of system (see Supporting Information for more details).
(36) Brenner, D. W.; Shenderova, O. A.; Harrison, J. A.; Stuart, S. J.; Ni, B.; Sinnott, S. B. *J. Phys.: Condens. Matter* **2002**, *14*, 783.
(37) Ouyang, M.; Huang, J. L.; Cheung, C. L.; Lieber, C. M. *Science* **2001**, *292*, 702.
(38) Park, N.; Miyamoto, Y.; Lee, K.; Choi, W. I.; Ihm, J.; Yu, J.; Han, S. W. *Chem. Phys. Lett.* **2005**, *403*, 135.
(39) Ren, Z. F. *Nat. Nanotechnol.* **2006**, *2*, 17.
(40) Smalley, R. E.; Li, Y. B, Moore, V. C.; Katherine Price, B.; Colorado, R.; Schmidt, H. K.; Hauge, R. H.; Barron, A. R.; Tour, J. M. *J. Am. Chem. Soc.* **2006**, *128*, 158234.
(41) Hod, O.; Barone, V.; Peralta, J. E.; Scuseria, G. E. *Nano Lett.* **2007**, *7*, 2295.

NL071613D